CORROSION SCIENCE AND TECHNOLOGY, Vol.23, No.4(2024), pp.266~277 pISSN 1598-6462 / eISSN 2288-6524
[Research Paper] DOI: https://doi.org/10.14773/cst.2024.23.4.266

Improvement of Chloride Induced Stress Corrosion Cracking Resistance of Welded 304L Stainless Steel by Ultrasonic Shot Peening

Hyunhak Cho[1], Young Ran Yoo[2], and Young Sik Kim[1,2,†]

[1]*Department of Materials Science and Engineering, Andong National University, 1375 Gyeongdong-ro, Andong 36729, South Korea*
[2]*Materials Research Centre for Energy and Clean Technology, Andong National University, 1375 Gyeongdong-ro, Andong 36729, South Korea*

(Received July 10, 2024; Revised July 31, 2024; Accepted July 31, 2024)

Due to its good corrosion and heat resistance with excellent mechanical properties, 304L stainless steel is commonly used in the fabrication of spent nuclear fuel dry storage canisters. However, welds are sensitive to stress corrosion cracking (SCC) due to residual stress generation. Although SCC resistance can be improved by stress relieving the weld and changing the chloride environment, it is difficult to change corrosion environment for certain applications. Stress control in the weld can improve SCC resistance. Ultrasonic shot peening (USP) needs further research as compressive residual stresses and microstructure changes due to plastic deformation may play a role in improving SCC resistance. In this study, 304L stainless steel was welded to generate residual stresses and exposed to a chloride environment after USP treatment to improve SCC properties. Effects of USP on SCC resistance and crack growth of specimens with compressive residual stresses generated more than 1 mm from the surface were studied. In addition, correlations of compressive residual stress, grain size, intergranular corrosion properties, and pitting potential with crack propagation rate were determined and the improvement of SCC properties by USP was analyzed.

Keywords: *Stainless steel, USP, GTAW, SCC, Microstructure*

1. Introduction

Austenitic stainless steel is a key material in the industrial sector and is used in nuclear power plants, petrochemical, plant industries, heat exchangers, architectural structures and domestic applications. The reason is that austenitic stainless steels possess outstanding corrosion resistance, mechanical strength, and weldability [1,2]. Because of these properties, 304L stainless steel is also used for applications such as storing spent nuclear fuels in dry storage canisters and as a protective barrier for steam generators in light water reactors for nuclear power plant [1]. However, austenitic stainless steels with excellent corrosion resistance are susceptible to corrosion and SCC in chloride solutions [2].

Spent nuclear fuel dry storage canisters are assembled by welding, and the welds are susceptible to stress corrosion cracking due to tensile residual stresses generated during solidification [3]. Stress corrosion cracking in welds is caused by the combination of tensile residual stresses and allowable material and corrosion environments, which significantly reduces lifetime. A recent study reported that SCC resistance can be improved by removing tensile residual stresses in the welds or by changing the chloride environment. However, since the corrosion environment cannot be altered to suit a specific application, controlling the tensile residual stress in the welds can effectively improve SCC resistance [1].

Recently, modifications to surface properties have been attempted to improve SCC resistance, such as shot peening (SP) [4,5], laser shock peening (LSP) [6,7], water jet peening (WJP) [8], USP [9-11], and ultrasonic nanocrystalline surface modification (UNSM) [12,13]. The surface of the material is plastically deformed by the surface modification method and the tensile residual stress is changed to compressive residual stress, which can refine the surface grain and improve the surface properties. It has been reported that the refinement of surface grains can inhibit corrosion by reducing interatomic distances, promoting interatomic diffusion, and keeping the formation of passivation films [14]. However, it is important to consider that the surface of the material has been roughened by the peening process, which is not uniform and can cause overlaps to act as corrosion initiation sites if present [15].

We recently analyzed the effect of LSP on the SCC properties of 304L stainless steel and reported the following main findings. The 304L stainless steel after LSP treatment

[†]Corresponding author: yikim@anu.ac.kr
HyunHak Cho: Ph.D. Candidate, Young-Ran Yoo: Senior Researcher, Young-Sik Kim: Professor

develops compressive residual stresses in the depth direction. It induced grain refinement in the cross-section and an increase in pitting potential, which reduced the gross crack propagation rate and net crack propagation rate by U-bend SCC test. However, in the case of intergranular corrosion properties or pitting potential of the surface and crack growth rate, the correlation between the properties were weak [14]. Laser shot peening with these results is considered to have low productivity, high process unit costs, and equipment set-up and environmental limitations [10]. The ultrasonic peening process is advantageous for the peening treatment of welds due to its productivity, economy, mobility and good working conditions [10,16].

USP is a technique that applies compressive stress to modify the mechanical properties of a material surface. The method comprises striking balls made of metal, glass, ceramic, etc. at high speeds using ultrasonic waves to produce plastic deformation on the surface of the material and converting the existing tensile stress into compressive stress [16]. USP treatment can improve the material's physical and mechanical properties, such as the surface hardness, corrosion and wear of the material, and increase the fatigue strength, which can extend the fatigue lifetime [1]. The advantages of ultrasonic peening have been recognized in previous studies and literature, and Malaki and Ding *et al*. report that ultrasonic peening is a suitable method for post-processing welded structures [10]. Our research group studied the effect of USP treatment on the microstructure and corrosion properties of 304L stainless steel and its welds. The USP treatment produced compressive residual stresses up to 1 mm from the surface, which increased the cross-sectional pitting potential and passivation resistance due to increased hardness and grain refinement [3]. Also, Ling and Ma *et al*. reported that a hard layer on the top surface with ultra-fine grains after ultrasonic peening on TIG-welded SS304 improves SCC resistance [17]. These studies reported that compressive residual stresses and microstructure changes due to plastic deformation were important in improving SCC resistance [1].

As discussed above, recent studies have shown excellent results from surface treatments, but few have improved the resistance of SCC to compressive stresses applied to a depth of 1 mm from the surface by USP treatments. Additionally, there is a lack of research on the effects of SCC initiation and propagation in welds and its correlation with crack growth and properties.

In this study, 304L stainless steel used in the fabrication of spent nuclear fuel dry storage vessels was gas tungsten arc welding (GTAW) welded to generate residual stresses and exposed to a chloride environment. The exposed specimens were USP treated to welded 304L stainless steel to improve SCC properties in a chloride environment. The effect of USP treatment on SCC resistance and crack growth was studied after the generation of compressive residual stresses more than 1 mm from the surface.

2. Experimental Methods

2.1. Specimen

The primary material used in this study is commercial 304L stainless steel (designated 304LB) [3]. The specimen was welded using the GTAW method, and the welded specimen was designated 304LW [3]. Table 1 provides the detailed chemical compositions of both the base material and the

Table 1. Chemical composition of 304L stainless steel and filler metal (wt%) [3]

	-	C	Cr	Ni	Mn	Si	Cu	Mo	Co	P	N	S	Cb+Ta	Fe
304L	-	0.02	18.6	9.6	1.65	0.47	-	-	0.03	0.022	0.07	0.03	-	Bal.
ER308L	Spec.	≤0.03	19.5-22.0	9.0-11.0	1.0-2.5	0.30-0.65	≤0.75	≤0.75	-	≤0.03	-	≤0.03	-	Bal.
	analysis	0.015	19.81	9.84	1.69	0.35	0.12	0.05	0.03	0.024	0.04	0.03	0.01	Bal.

Table 2. Welding parameters of the experimental specimen [3]

Welding Process	Current (A)	Voltage (V)	Speed (cm/min)	Shield Gas (%)	Groove Angle (°)	Welding Electrode
GTAW	245~250	14~15	9~10	Ar. 99.9	15	ER308L (Dia. 0.9 mm wire)

Table 3. Designation of the experimental specimen [3]

Alloy		Non-peened	Ultrasonic Shot Peened
304L	Base metal	304LB	304LB-USP
	Weldment	304LW-W	304LW-W-USP

Table 4. Conditions of ultrasonic shot peening processing [1]

Specimen Type	Manufacturer	Media	Frequency (kHz)	Beads Material
Base metal and Welded specimen	SONATS Stress voyager	Air	20	304L
Medium Diameter (mm)	Beads Weight (g)	Amplitude (μm)	Peening Duration (Min.)	Coverage rate
4	25.5	70	3	>100%

ER308L filler metal utilized in this study. The welding was performed using 25 mm thick 304L stainless steel as the base material, with a groove angle of 15°. The parameters of the welding process are outlined in Table 2, while Table 3 summarizes the samples from the base metal, heat-affected zone (HAZ), and weld metal.

2.2. USP treatment

The USP process employed technology developed by SONATS in France [18]. The peening was conducted at a frequency of 20 kHz, utilizing media with a diameter of 4 mm, an amplitude of 70 μm, for a duration of 3 minutes, and achieving a coverage rate of over 100%. Table 4 details the specific peening conditions. USP involves surface peening by transferring ultrasonic vibrations to the media. The specimen was positioned with the target area facing downward, making contact with the medium in the chamber, resulting in a shot-peened specimen [19,20].

2.3. U-Bend SCC Test

U-bend specimens for SCC testing were prepared in accordance with ASTM G 30 (size d) [21]. Welded specimens were prepared in accordance with ASTM G58 [22].

The SCC test was conducted in accordance with ASTM G36 [23], using 42% $MgCl_2$ at a boiling temperature of 155 °C as the test solution. During the test, the U-bend areas were observed at intervals of 1.5 or 3 hours. Fig. 1 shows (a) the corrosion cell for SCC testing of U-bend specimens, (b) the side insulation of the U-bend specimen, and (c) the setup of the U-bend specimen. The insulation was applied with a high-temperature adhesive (Original Cold-Weld, JB WELD, Georgia, USA) to prevent cracking in the peened area.

The SCC resistance was evaluated by "Total Crack Time" and "Crack Initiation Time". Total crack time refers to the time when cracks were observed through observations at regular intervals. Crack initiation time refers to the last time that no cracks were observed through the observations at a certain interval, from which the crack initiation time was estimated. An optical microscope was used to observe cracks in a specimen cross-section after SCC testing. The specimen cross-sections were polished with #2,000 SiC paper and polished with diamond paste (3 μm). The polished specimens were etched using an electrochemical etching device (Lectropol-5, Struers, France) in 10% oxalic acid. An optical microscope was used to examine the surface of the etched specimen (Axiotech 100HD, ZEISS, Oberkochen, Germany)

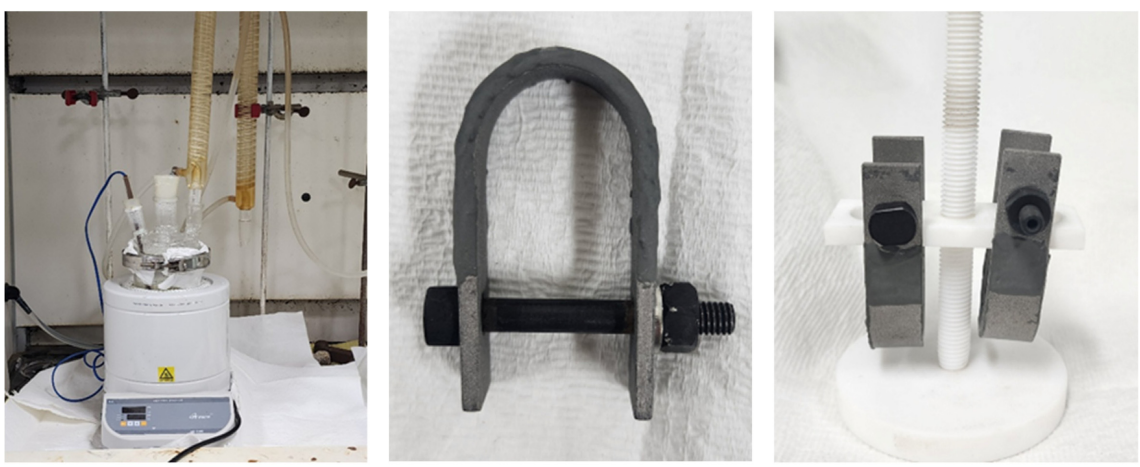

(a) (b) (c)

Fig. 1. (a) Corrosion Test Cell for U-Bend SCC Test; (b) Side Insulation of U-Bended Specimen; (c) Preparation of U-Bend Specimen

and the linear crack length was measured [14]. The crack propagation velocity was calculated by the equation below [14]. In addition, crack mode was observed using a SEM (VEGA ll LMU, Tescan, Czech Republic).

Total Crack Propagation Rate = Crack Length / Total Crack Time

Net Crack Propagation Rate = Crack Length / (Total Crack Time - Crack Initiation Time)

2.4. Microstructure Analysis

The specimens were prepared by cutting to dimensions of 15 × 15 × 10 mm, polishing with #2000 SiC paper, and then polishing with 3 μm diamond paste. It was etched using an electrolytic etcher (Lectropol-5, Struers, France) in a 10% oxalic acid solution (consisting of 100 g $H_2C_2O_4$-$2H_2O$ in 900 ml distilled water). After etching, the specimens were cleaned with ethyl alcohol using an ultrasonic cleaner. Subsequently, the microstructure was examined using an optical microscope (AXIOTECH 100HD, ZEISS, Oberkochen, Germany). The average grain size was calculated for the cross-section of the peened specimen using the ASTM E1382 method [24].

Surface observation and compositional analysis, the SEM photographed specimen was cut to a size of 15 × 15 mm, and in the case of the USP treated specimen, SEM-EDS was photographed without surface polishing. The surface morphology was observed by SEM (VEGA II LMU, Tescan, Brno, Czech Republic).

2.5. Residual Stress Measurement

The specimen's surface residual stress was measured using the hole drilling method (RS-200 Assembly, VMM, Raleigh, NC, USA). After attaching a strain gauge (CEA 06 062UL 12, VMM, Raleigh, NC, USA) to the specimen, a hole was drilled using a drilling device and the residual stresses released during the drilling process were measured. The residual stress of the bending specimen was measured in the apex area of the peened specimen.

3. Results

3.1 Effect of Ultrasonic Shot Peening on SCC of 304L Stainless Steel

Fig. 2 shows surface and cross-sectional observations of 304LB stainless steel before and after crack generating by the USP treatment. In Fig. 2a, Before U-Bend SCC Test shows the image before U-Bend test at 155 °C, 42% $MgCl_2$ condition. And After Test shows the surface image after U-Bend test, and Cross-Section After Test shows the image of the cross-section after cracking by U-Bend test. The red boxes in the figure indicate the areas where cracks were observed, and it can be observed that both specimens cracked at the apex of the specimen.

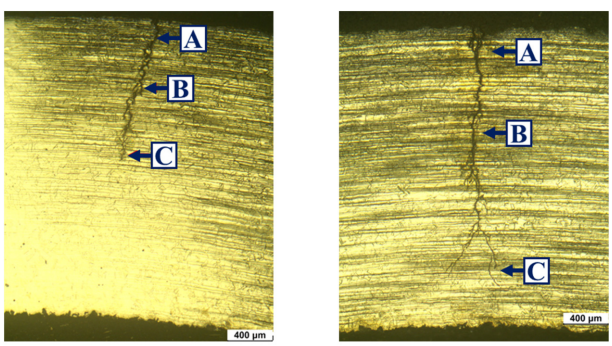

Fig. 3. Images of the cross-section of U-bended 304LB after SCC test (OM, ×50, 42% $MgCl_2$ at 155 °C): (a) 304LB (Non-peened) and (b) 304LB (USP)

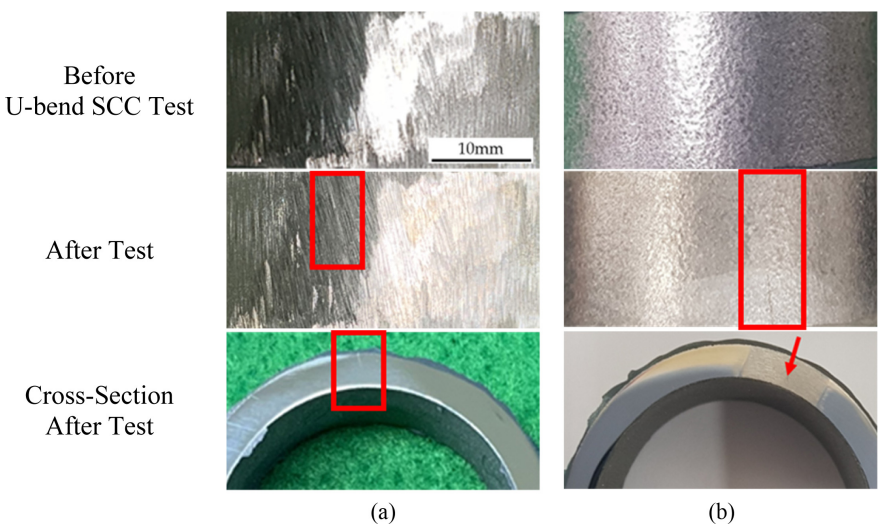

Fig. 2. Surface appearance of 304LB by USP: (a) 304LB (non-peened) and (b) 304LB (USP)

Fig. 3 shows the crack in 304LB after the U-Bend SCC test. Fig. 3a shows the crack in 304LB, and Fig. 3b shows the crack in 304LB-USP. The red marked area in Fig. 3 was observed at high magnification as shown in Fig. 4, which shows the crack morphology of 304LB after the U-Bend SCC test. The non-Peened 304LB specimen shows mixed cracking mode (intergranular and transgranular cracking), while the 304LB-USP specimen shows transgranular cracking. To confirm the crack mode, the cracked specimen was fractured and the fractured surface was observed, as shown in Fig. 5, which shows the crack mode of U-bended 304LB after SCC test. The images of all specimens show cracks that are primarily observed in optical microscopy and show the intergranular crack mode.

Fig. 6 shows the effect of peening on crack time for U-Bend SCC test results for USP-treated 304LB stainless steel at 155 °C, 42% $MgCl_2$. Fig. 6a shows the results of total crack time and crack initiation time, 304LB had a total crack time

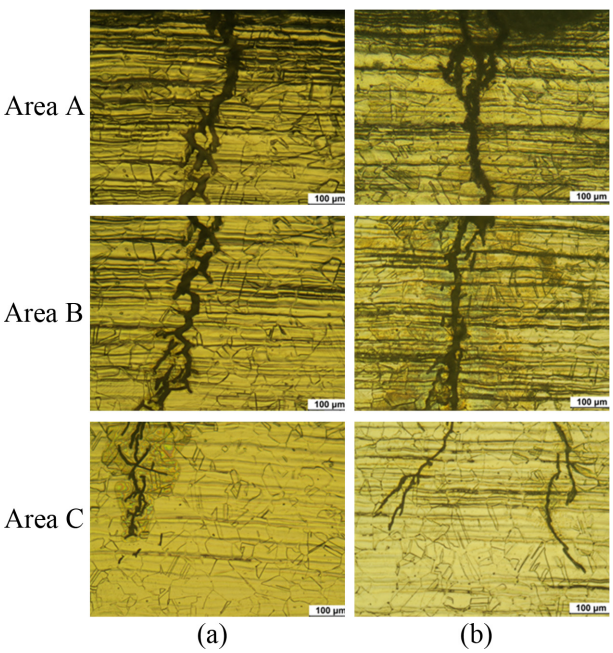

Fig. 4. Crack morphologies of U-bended 304LB after SCC test (OM, ×200, 42% $MgCl_2$ at 155 °C, Area A, B, C in Fig. 4): (a) 304LB (Non-peened) and (b) 304LB (USP)

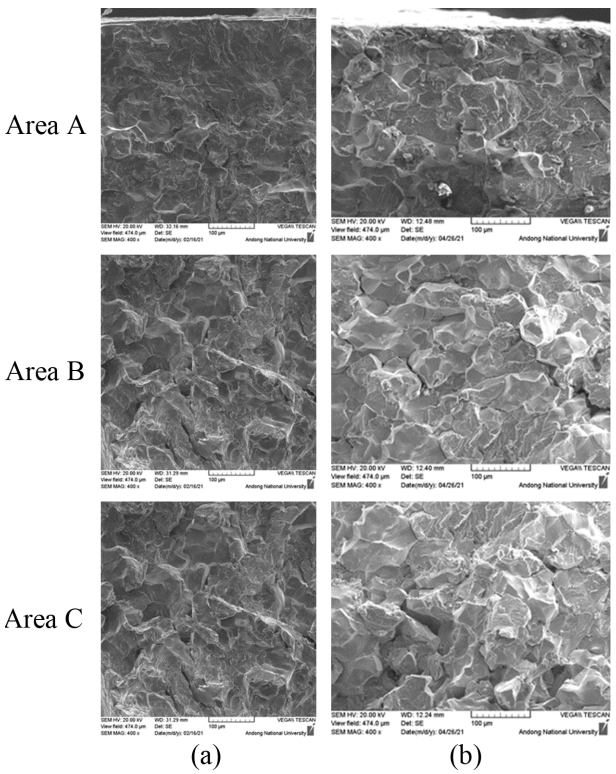

Fig. 5. Cracking mode of 304LB after U-Bend SCC test (SEM, ×400, 155 °C, 42% $MgCl_2$, Area A, B and C in Fig. 4 and 5): (a) 304LB (Non-peened) and (b) 304LB (USP)

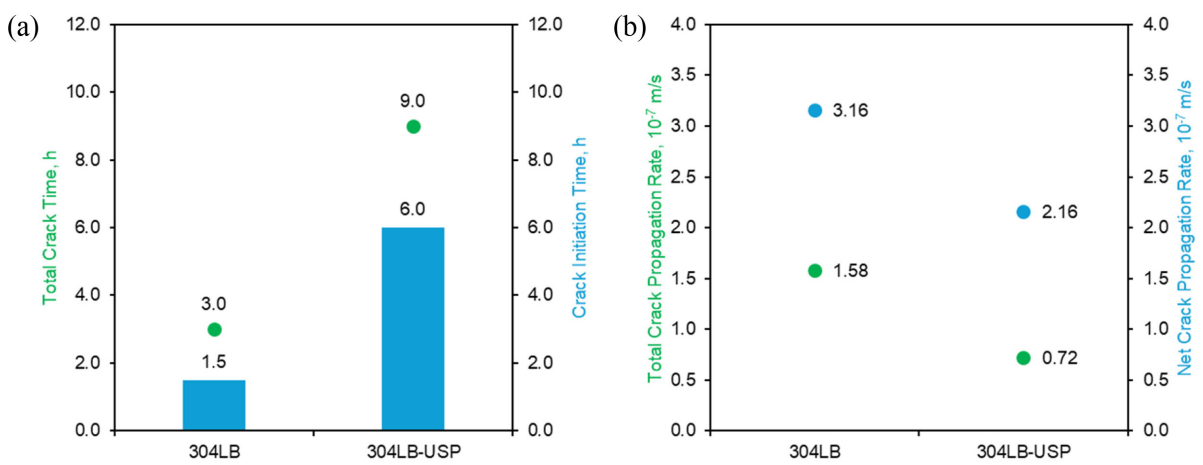

Fig. 6. Effect of USP on the crack times of U-bended 304LB by SCC test in 155 °C, 42% $MgCl_2$: (a) crack time and (b) crack propagation rates

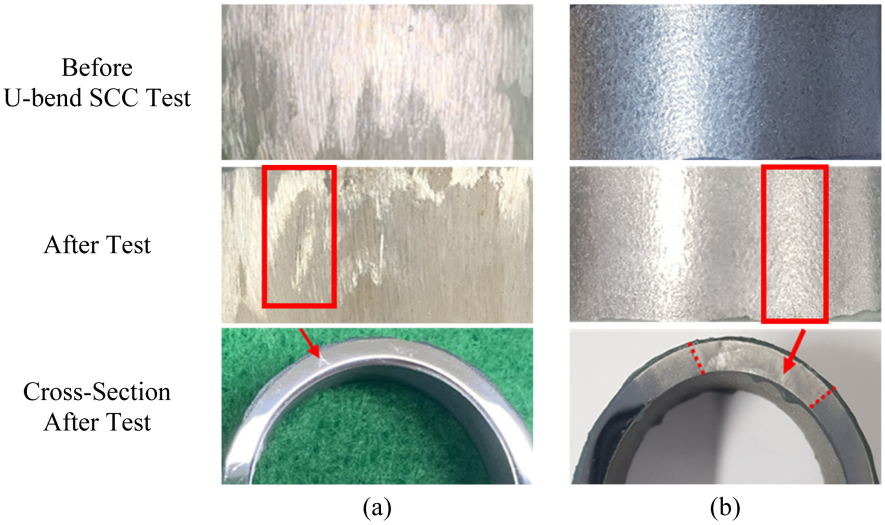

Fig. 7. Surface appearance of 304LW by USP: (a) 304LW (Non-peened) and (b) 304LW (USP)

of 3 hours and crack initiation time of 1.5 hours, while 304LB-USP had a total crack time of 9 hours and crack initiation time of 6 hours. Fig. 6b shows the crack growth rate depending on the crack length and crack time. The 304LB was measured to have a total crack growth rate of 1.58×10^{-7}m/s and a crack growth rate after crack initiation of 3.16×10^{-7}m/s, while the 304LB-USP had a total crack growth rate of 0.72×10^{-7}m/s and a crack growth rate after crack initiation of 2.16×10^{-7}m/s. The USP treatment can slow the crack growth time and crack initiation time. It can also reduce the total crack growth rate and the growth rate after crack initiation.

3.2 Effect of Ultrasonic Shot Peening on SCC of Welded 304L Stainless Steel

Fig. 7 shows images of surface and cross-section observations of 304LW stainless steel after USP. Fig. 7a shows apex and cross-section images of 304LW before and after the U-Bend SCC Test, while Fig. 7b shows apex and cross-sectional images of 304LW-USP. After the U-Bend test, a crack was formed in the apex area of the specimen and was observed in the cross-section of the specimen. In Fig. 7, the red color area and arrows indicate where the cracks were observed.

Fig. 8 shows the crack morphology of 304LW after the U-Bend SCC test. Fig. 8a shows the crack in 304LW and Fig. 8b depicts the crack in 304LW-USP. The image observed at high magnification for the red marked area where the crack occurred in Fig. 8 is shown in Fig. 9 and shows the crack morphology of U-bended 304LW after the SCC test (Areas A, B and C in Fig. 8). The non-peened 304LW specimen

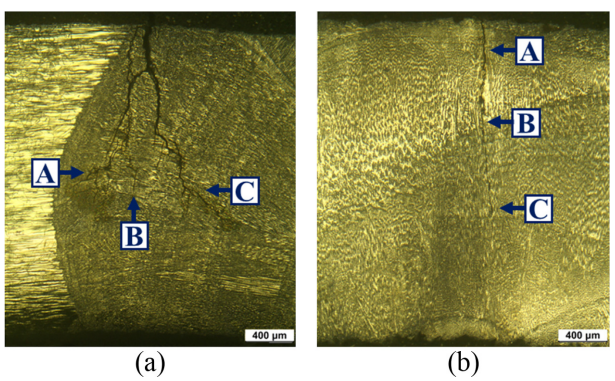

Fig. 8. Images of the cross-section of U-bended 304LW after SCC test (OM, ×50, 42% $MgCl_2$ at 155 °C): (a) 304LW (Non-peened) and (b) 304LW (USP)

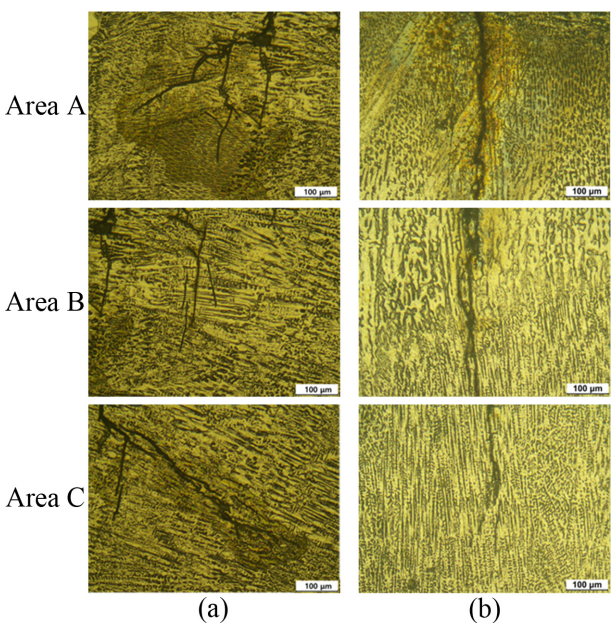

Fig. 9. Crack morphologies of U-bended 304LW after SCC test (OM, ×200, 42% $MgCl_2$ at 155 °C, Area A, B and C in Fig. 8): (a) 304LW (Non-peened) and (b) 304LW (USP)

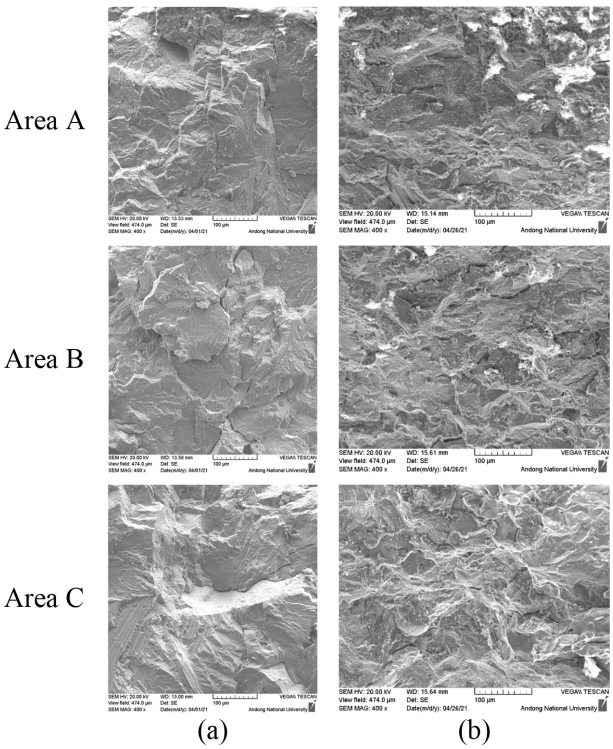

Fig. 10. Cracking mode of U-bended 304LW after SCC test (SEM, ×400, 42% $MgCl_2$ at 155 °C, Area A, B and C in Fig. 8): (a) 304LW (Non-peened) and (b) 304LW (USP)

shows the form of transgranular cracks, and the 304LW-USP specimen also shows the form of transgranular cracks. To confirm the crack mode, the cracked specimen was fractured and the fractured surface was observed, as shown in Fig. 10, which shows the crack mode of 304LW after U-Bend SCC test (SEM ×400, 155 °C, 42% $MgCl_2$). The images of all specimens, regardless of peening, show cracks that are primarily observed in optical microscopy and show the intergranular crack mode.

Fig. 11 shows the effect of USP on crack time after U-Bend SCC test (155 °C, 42% $MgCl_2$) of a welded 304LW specimen. Fig. 11a shows the results of total crack time and crack initiation time, non-peened 304LW had a total crack time of 3 hours and crack initiation time of 1.5 hours, while USP treated 304LW-USP had a total crack time of 6 hours and crack initiation time of 3 hours. The total crack time and crack initiation time of welded 304LW increased about doubled after peening treatment. Fig. 11b shows the effect of USP on crack propagation rate after U-Bend SCC test (155 °C, 42% $MgCl_2$) of welded 304LW specimen. The total crack growth rate is 1.53×10^{-7}m/s for 304LW and 0.82×10^{-7}m/s for 304LW-USP. In addition, the crack growth rate after crack initiation is 3.07×10^{-7}m/s for 304LW and 1.64×10^{-7}m/s for 304LB-USP. These results show that USP treatment of the welded 304LW surface reduced both crack time and crack initiation time, and that USP can reduce the total crack growth rate and crack growth rate after crack initiation of welded 304L stainless steel in a chloride environment.

4. Discussion

The compressive residual stresses added to the surface of 304L stainless steel by the USP treatment caused the outermost surface grains to refine and changed corrosion properties. In addition, the correlation between corrosion properties and stress corrosion cracking was also confirmed, and Fig. 12 shows the correlation between crack propagation rate and surface residual stress in the base metal and welds of 304L stainless steel by USP. The surface residual stresses were obtained by the hole drilling method as described in previous research literature [3]. The non-peened 304L stainless steel shows tensile residual stresses at the surface

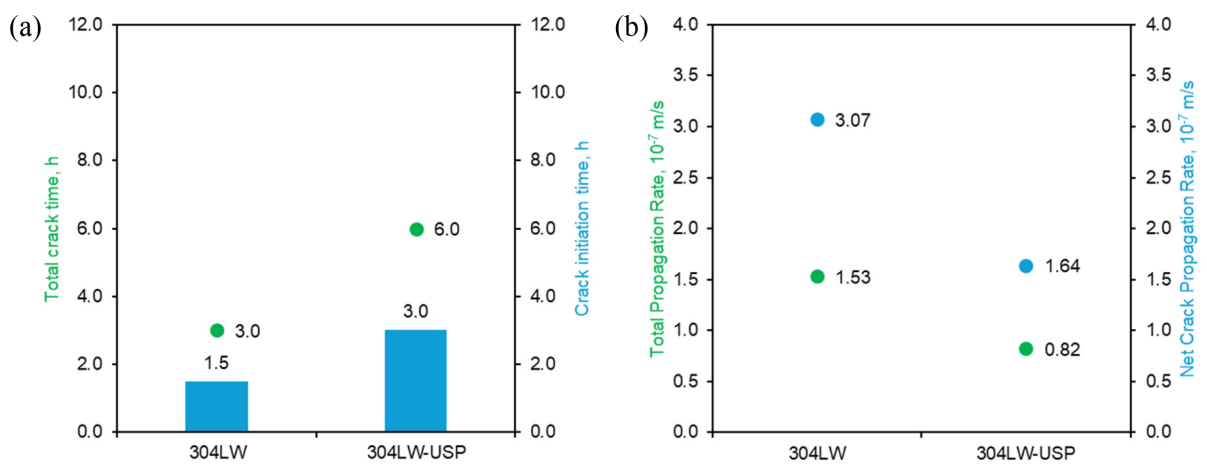

Fig. 11. Effect of USP on the crack times of U-bended 304LW after SCC test in 155 °C, 42% $MgCl_2$; (a) crack time and (b) crack propagation rates

and 1 mm depth, while the USP-treated specimen shows compressive residual stresses regardless of the measurement location. Fig. 12a shows the correlation between total crack propagation rate and residual stress, which shows that the total crack propagation rate decreases with increasing compressive residual stress, but the total crack propagation rate increases with increasing tensile residual stress. The trend is the same for the correlation of net crack propagation rate with residual stress in Fig. 12b. The USP treatment increased SCC resistance in the chloride environment because the 304L stainless steel internal compressive residual stresses and increased pitting resistance [14,25].

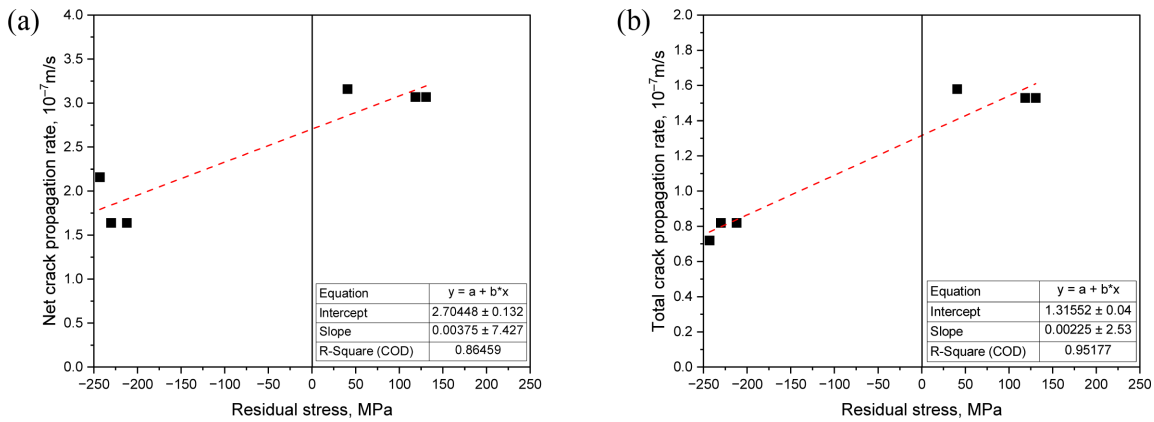

Fig. 12. Correlation between the crack propagation rate and residual stress: (a) total crack propagation and (b) net crack propagation rate

Table 5. The average grain size and corrosion parameters of 304L base and welded metals by peening [3]

Peening Condition		Average Grain Size*, µm	DOS**, I_r/I_a	IGC Rate***, mm/y	E_p****, V(SCE) of Surface	E_p*****, V(SCE) of Cross-Section
Non-peened	Base metal	23.73	0.00003	0.12	0.935	0.310
	HAZ	26.02	0.00095	0.20	1.030	0.217
	Weldment	-	0.00104		0.789	0.065
USP	Base metal	13.76	0.01300	0.29	0.365	0.950
	HAZ	15.41	0.01100	0.19	0.254	0.046
	Weldment	-	0.01200		-0.115	0.528

*Average Grain Size [3], ** DOS [3], *** IGC Rate [3], **** E_p (Surface) [3], ***** E_p (Cross-Section) [3]

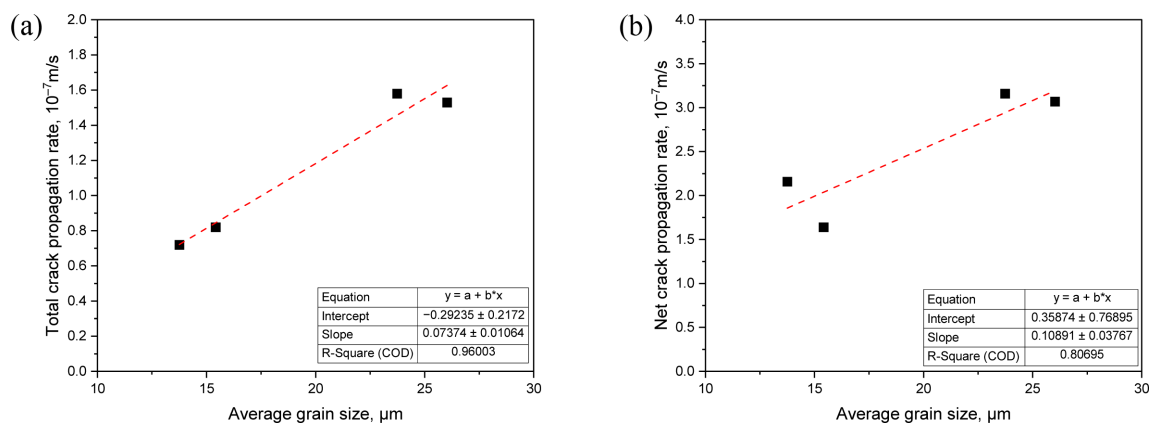

Fig. 13. Correlation between the total and net crack propagation rate and average grain size: (a) total crack propagation rate and (b) net crack propagation rate

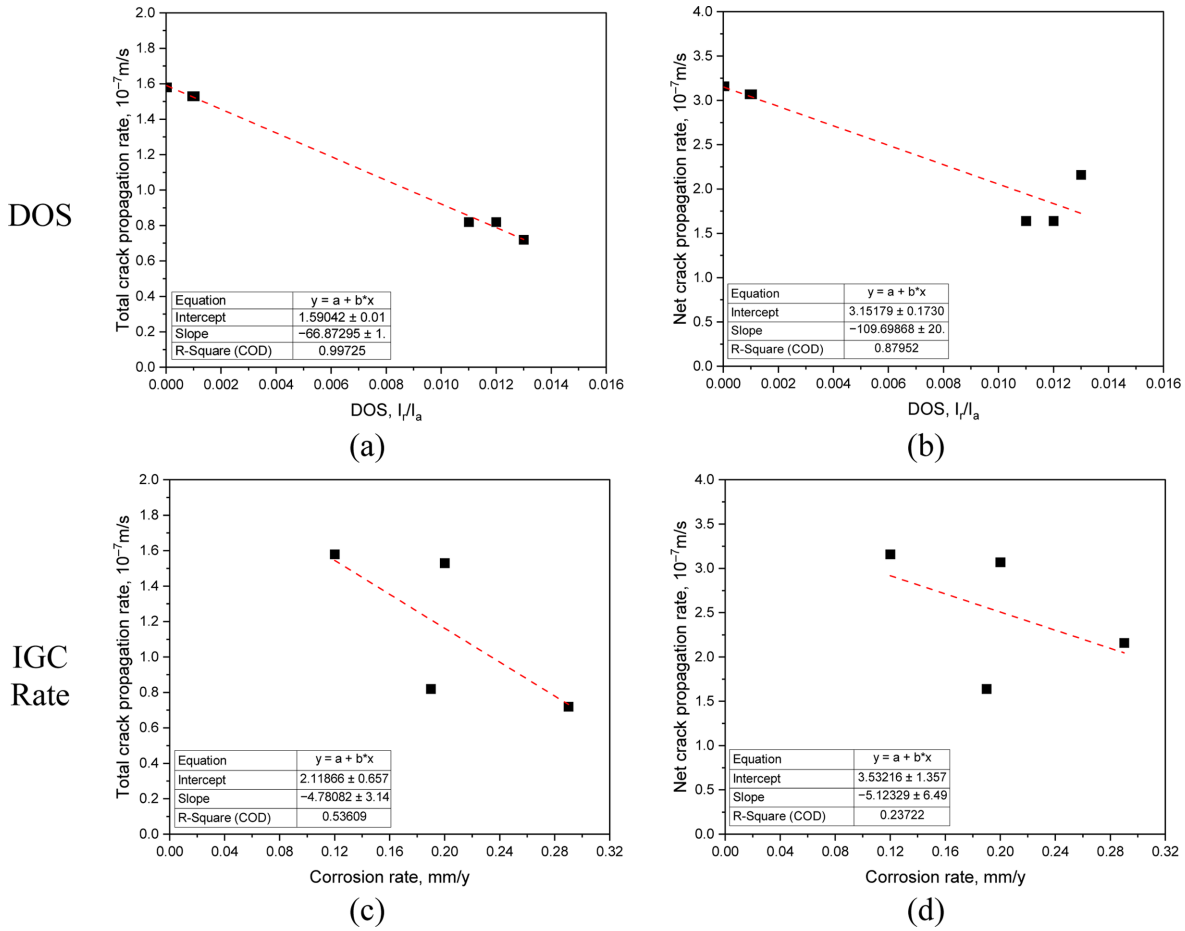

Fig. 14. Correlation between crack propagation rate and intergranular corrosion: (a, c) total crack propagation and (b, d) net crack propagation rate

The effect of USP treatment of 304L stainless steel was reported in a previous study to roughen the surface while refining the grains in the outermost area [3,26]. Table 5 lists the average micronized grain size and corrosion properties of 304L stainless steel by USP. The values in Table 5 show the correlation between microstructure and corrosion properties and crack propagation rate. Fig. 13 shows the correlation between average grain size and crack propagation rate, with the total crack propagation rate increasing as the average grain size increases. Also, the net crack propagation rate is increasing as the average grain size increases, therefore it can be seen that grain size affects crack propagation [27,28].

In a previous study, the intergranular corrosion rate of USP-treated specimens was higher than non-peened specimens [3]. The micronized grains by USP increased the intergranular corrosion rate due to the increase in grain boundary area. Fig. 14 shows correlation between intergranular corrosion rate and crack propagation rate, with total crack propagation rate and net crack propagation rate reduced as the DOS increased. In addition, the total crack propagation rate and net crack propagation rate reduced as the intergranular corrosion rate increased. The observations in Fig.s 4, 5, 9 and 10 confirm the intergranular crack morphology, which indicates that intergranular corrosion properties did not significantly affect the SCC of 304L stainless steel. The effects of welds and USP treatment are also not significant.

Fig. 15 shows the correlation between crack propagation rate and pitting potential for 304L stainless steel. Fig.s 15a and 15b are the correlation of the crack propagation rate and the surface pitting potential, which shows that the crack propagation rate increases as the pitting potential of the surface increases. Fig.s 15c and 15d are the correlation of crack propagation rate and pitting potential of the cross-section, which shows that the crack propagation rate decreased as the pitting potential increased. These results can be considered in relation to USP-induced microstructural changes, as confirmed in previous studies. As described in previous literature [3], USP increased the surface roughness of 304L stainless steel, which reduced the pitting potential. The cross-section, on the other hand, increased the pitting potential by

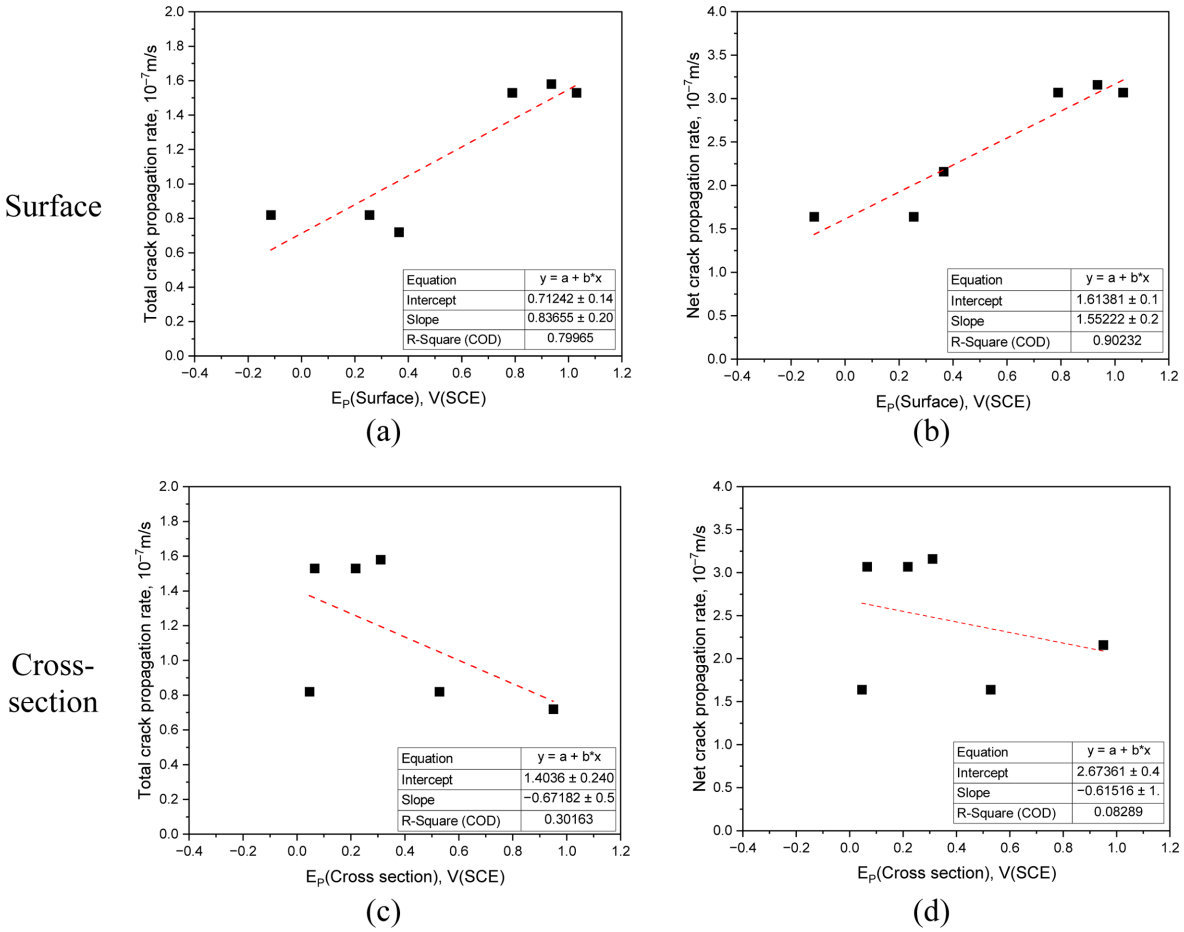

Fig. 15. Correlation between the crack propagation rate and pitting potential [3]: (a, c) total crack propagation and (b, d) net crack propagation rate

Table 6. Ultrasonic shot peening effect on the estimated SCC initiation time and SCC Propagation of 304L stainless steel in boiling 42% $MgCl_2$

Specimen		Base metal	Welded metal
Estimated Crack Initiation Time, hrs	Non-Peened	1.5	1.5
	Peened	6	3
	Peening Effect, %	300 (Beneficial)	100 (Beneficial)
Net Crack Propagation Rate × 10^{-7}, m/s	Non-Peened	3.16	3.07
	Peened	2.16	1.64
	Peening Effect, %	-31.6 (Beneficial)	-46.6 (Beneficial)

refinement of the outermost grains. These properties are shown in Fig. 15, which indicates that the SCC resistance of 304L stainless steel was affected by the corrosion properties of the cross-section grain refinement rather than the corrosion properties of the surface by USP, which affected the crack propagation rate.

Table 6 shows a summary of the SCC initiation times and net crack propagation rates for 304L stainless steel measured in Fig.s 6 and 11. The USP increased the crack initiation time for both the base material and the weld, with the base material showing a greater increase in crack initiation time than the weld. The improvement in crack initiation time on SCC by

USP is 100% or more based on time. The USP reduced the crack propagation rate in 304L stainless steel, regardless of the base metal and welds. The effect of USP on SCC resistance was compared by crack propagation rate, which was reduced by 31.6% for the base metal and 46.6% for the welds.

5. Conclusions

This study evaluated the effect of USP on the SCC properties of welded 304L stainless steel. The effects and correlations of changes in microstructure, corrosion properties, and residual stress on SCC by USP treatment were analyzed and the following conclusions were obtained.

(1) The U-Bend SCC properties of 304L stainless steel are characterized by USP treatment, which increases the initial crack initiation time and total crack time but decreases the crack growth rate after crack initiation. This is due to the compressive residual stresses added to the surface by USP, which causes fine grains to delay crack initiation and reduce the crack growth rate, thus improving the SCC properties.

(2) The properties of U-Bend SCC by USP treatment are correlated with compressive residual stress and grain refinement, but lack correlation with corrosion properties, especially surface pitting and intergranular corrosion properties.

Acknowledgments

This research was supported by a grant from the 2023-2024 research funds of Andong National University.

References

1. M. John, A. M. Ralls, M. Misra, and P. L. Menezes, Effect of ultrasonic impact peening on stress corrosion cracking resistance of austenitic stainless-steel welds for nuclear canister applications, *Journal of Nuclear Materials*, **584**, 154590 (2023). Doi: https://doi.org/10.1016/j.jnucmat.2023.154590
2. T. Ahn, G. Oberson and S. DePaula, *ECS Transactions*, p. 211, The Electrochemical Society, Washington, USA (2013). Doi: https://doi.org/10.1149/05031.0211ecst
3. H. H. Cho, Y. R. Yoo, and Y. S. Kim, Effect of Ultrasonic Shot Peening on Microstructure and Corrosion Properties of GTA-Welded 304L Stainless Steel, *Crystals*, **14**, 531 (2024). Doi: https://doi.org/10.3390/cryst14060531
4. W. T. Tsai, C. S. Chang, and J. T. Lee, Effects of Shot Peening on Corrosion and Stress Corrosion Cracking Behaviors of Sensitized Alloy 600 in Thiosulfate Solution, *Corrosion Science*, **50**, 98 (1994). Doi: https://doi.org/10.5006/1.3293507
5. T. Wang, J. Yu, and B. Dong, Surface Nano Crystallization Induced by Shot Peening and its Effect on Corrosion Resistance of 1Cr18Ni9Ti Stainless Steel, *Surface & Coating Technology*, **200**, 4777 (2006). Doi: https://doi.org/10.1016/j.surfcoat.2005.04.046
6. J. H. Kim, W. R. Lee, T. G. Kim, and S. K. Cheong, *Transactions of the Korean Society of Mechanical Engineers B*, pp. 1041 – 1046, The Korean Society of Mechanical Engineers, Pusan, Korea (2011). Doi: http://dx.doi.org/10.3795/KSME-B.2011.35.10.1041
7. J. Z. Lu, H. Qi, K. Y. Luo, M. Luo, and X. N. Cheng, Corrosion Behaviour of AISI 304 Stainless Steel Subjected to Massive Laser Shock Peening Impacts with Different Pulse Energies, *Corrosion Science*, **80**, 53 (2014). Doi: https://doi.org/10.1016/j.corsci.2013.11.003
8. W. Jiang, Y. Luo, H. Wang, and B. Wang, Effect of impact pressure on reducing the weld residual stress by water jet peening in repair weld to 304 stainless steel clad plate, *Journal of Pressure Vessel Technology*, **137**, 031401 (2015). Doi: https://doi.org/10.1115/1.4029655
9. S. Amini, S. A. Kariman, and R. Teimouri, The Effects of Ultrasonic Peening on Chemical Corrosion Behavior of Aluminum 7075, *The International Journal of Advanced Manufacturing Technology,* **91**, 1091 (2017). Doi: https://doi.org/10.1007/s00170-016-9795-6
10. M. Malaki, and H. Ding, A Review of Ultrasonic Peening Treatment, *Materials and Design*, **87**, 1072 (2015). Doi: https://doi.org/10.1016/j.matdes.2015.08.102
11. S. Manchoul, R. B. Sghaier, R. Seddik, and R. Fathallah, Comparison Between Conventional Shot Peening and Ultrasonic Shot Peening, *Mechanics & Industry*, **19**, 603 (2018). Doi: https://doi.org/10.1051/meca/2018045
12. J. H. Lee, and Y. S. Kim, Intergranular Corrosion of 316L Stainless Steel by Aging and UNSM (Ultrasonic Nanocrystal Surface Modification) Treatment, *Corrosion Science and Technology*, **14**, 313 (2015). Doi: https://doi.org/10.14773/cst.2015.14.6.313
13. C. Ma, M. T. Andani, H. Qin, N. S. Moghaddam, H. Ibrahim, A. Jahadakbar, A. Amerinatanzi, Z. Ren, H. Zhang, G. L. Doll, Y. Dong, M. Elahinia, and C. Ye, Improving Surface Finish and Wear Resistance of Additive Manufactured Nickel-Titanium by Ultrasonic Nano-Crystal Surface Modification, *Journal of Materials Processing Technology*, **249**, 433 (2017). Doi: https://doi.org/

10.1016/j.jmatprotec.2017.06.038

14. Y. R. Yoo, S. H. Choi, and Y. S. Kim, Effect of Laser Shock Peening on the Stress Corrosion Cracking of 304L Stainless Steel, *Metals*, **13**, 516 (2023). Doi: https://doi.org/10.3390/met13030516
15. K. T. Kim, and Y. S. Kim, Effect of the amplitude in ultrasonic nano-crystalline surface modification on the corrosion properties of alloy 600, *Corrosion Science and Technology*, **18**, 196 (2019). Doi: https://doi.org/10.14773/cst.2019.18.5.196
16. V. Robin, P. Gilles, A. Brosse, and T. Chaise, *ASME 2015 Pressure Vessels and Piping Conference*, PVP2015-45973, ASME, Boston, USA (2015). Doi: https://doi.org/10.1115/PVP2015-45973
17. X. Ling, and G. Ma, Effect of Ultrasonic Impact Treatment on the Stress Corrosion Cracking of 304 Stainless Steel Welded Joints, *Journal of Pressure Vessel Technology*, **131**, 051502 (2009). Doi: https://doi.org/10.1115/1.3147988
18. SONATS.Available online: https://sonats-et.com/en/ (accessed on 4 January 2024).
19. F. Yin, M. Rakita, S. Hu, and Q. Han, Overview of Ultrasonic Shot Peening. *Surface Engineering*, **33**, 651 (2017). Doi: https://doi.org/10.1080/02670844.2017.1278838
20. Q. Zhang, B. Duan, Z. Zhang, J. Wang, and C. Si, Effect of Ultrasonic Shot Peening on Microstructure Evolution and Corrosion Resistance of Selective Laser Melted Ti-6Al-4V Alloy, *Journal of Materials Research and Technology*, **11**, 1090 (2011). Doi: https://doi.org/10.1016/j.jmrt.2021.01.091
21. ASTM G30-2003, Standard Practice for Making and Using U-Bend Stress-Corrosion Test Specimens. ASTM International, West Conshohocken, PA, USA (2003).
22. ASTM G58-2015, Standard Practice for Preparation of Stress-Corrosion Test Specimens for Weldments. ASTM International, West Conshohocken, PA, USA (2015).
23. ASTM G36-2000, Standard Practice for Evaluating Stress-Corrosion-Cracking Resistance of Metals and Alloys in a Boiling Magnesium Chloride Solution. ASTM International, West Conshohocken, PA, USA (2000).
24. ASTME 1382, Standard Test Method for Determining Average Grain Size Using Semiautomatic and Automatic Image Analysis. ASTM International, West Conshohocken, PA, USA (2015).
25. J. Z. Lu, K. Y Luo, D. K. Yang, X. N. Cheng, J. L. Hu, F. Z. Dai, H. Qi, L. Zhang, J. S. Zhong, Q. W. Wang, and Y. K. Zhang, Effects of laser peening on stress corrosion cracking (SCC) of ANSI 304 austenitic stainless steel, *Corrosion Science*, **60**, 145 (2012). Doi: http://dx.doi.org/10.1016/j.corsci.2012.03.044
26. G. Liu, J. Lu, and K. Lu, Surface Nanocrystallization of 316L Stainless Steel Induced by Ultrasonic Shot Peening, *Materials Science and Engineering: A*, **286**, 91 (2000). Doi: https://doi.org/10.1016/S0921-5093(00)00686-9
27. M. Banaszkiewicz, and A. Rehmus-Forc, Stress corrosion cracking of a 60 MW steam turbine rotor, *Engineering Failure Analysis*, **51**, 55 (2015). Doi: https://doi.org/10.1016/j.engfailanal.2015.02.015
28. H. F. Lopez, M. M. Cisneros, H. Mancha, O. Garcia, and M. J. Perez, Grain size effects on the SCC susceptibility of a nitrogen steel in hot NaCl solutions, *Corrosion Science*, **48**, 913 (2006). Doi: https://doi.org/10.1016/j.corsci.2005.02.017